Original research

Dual-energy X-ray absorptiometry (DXA) to measure bone mineral density (BMD) for diagnosis of osteoporosis - experimental data from artificial vertebrae confirms significant dependence on bone size

Paul Henry Golding

Unit 22 Hibiscus Nambour, 55 Carter Road, Nambour 4560, QLD, Australia

A B S T R A C T

Introduction: The WHO definition of osteoporosis, and published BMD (Bone Mineral Density) references ranges, do not consider differences in bone size. Because it is a two-dimensional technique, and cannot measure bone depth, aBMD (areal BMD) measured using DXA (Dual-energy X-Ray Absorptiometry) is affected by bone size variability. Mathematical models have been devised to correct aBMD for bone size, but these are confounded by variations in soft tissue surrounding bone. Confirmation of the actual quantitative effect on clinical results for patients requires precise changes in bone size and mineral density, but studies of humans and animals are limited by the inability to precisely control these in natural bones.
Purpose: The objectives of this experiment were to obtain precise, repeatable, quantitative data from sets of artificial vertebrae to confirm the dependence of aBMD on bone size in clinical practice, and to test the effect of applying corrections based on assumptions that the vertebrae were simple geometric shapes to produce corrected BMAD (Bone Mineral Apparent Density).
Methods and materials: Four sets of artificial bones, each set containing four cylinders of different diameters but identical in height, were constructed by casting a mixture of epoxy resin and calcium carbonate powder into a mould. The cylinders were considered to be artificial vertebrae L1 to L4 so that all four in a set may be tested in a single scan. The X-Ray attenuation of the material used was varied between the sets, to represent differences in BMD. Each set of vertebrae was inserted into a soft-tissue analogue and DXA scanned, in the anteroposterior position, with the GE Lunar Prodigy and the Hologic Discovery.
Results: The results verify the theoretical direct proportionality between aBMD and diameter, confirming that aBMD is significantly affected by bone size. Applying a BMAD correction, by assuming the vertebrae to be cylinders, reduced the effect of change in bone diameter by approximately two orders of magnitude to an insignificant level.
Conclusion: This experiment has confirmed that BMD measured using DXA, accepted in clinical practice as the *"gold standard"* means of diagnosing osteoporosis, could lead to misdiagnosis because it is significantly affected by differences in bone size.

1. Introduction

1.1. Definition of osteoporosis, and references ranges, do not consider differences in bone size

The World Health Organization defines osteoporosis as having a BMD of 2.5 or more standard deviations below the mean value for young adults (WHO Scientific Group, 2007; WHO Scientific Group, 2003). Those WHO reports do not specify how differences in bone size should be taken into account when reporting BMD results.

Published reference ranges, obtained from studies of healthy volunteers, are for populations of limited diversity and do not take into account the effect of bone size differences on aBMD results. For example, Henry et al. (2010), cited in clinical results from the GE Lunar Prodigy DXA scanner in Australia, provides reference ranges of BMD for white males categorized by age group but not by bone size.

1.2. DXA BMD confounded by bone size variability

Bone size variability confounds results from DXA BMD, which

measures two-dimensional areal bone mineral density (aBMD) rather than true three-dimensional volumetric bone mineral density (vBMD). Two-dimensional imaging can be used to measure length and width but not bone depth. Several reviews of imaging methods for BMD have considered the ensuing problems associated with interpreting DXA results (Binkovitz and Henwood, 2007; Carter et al., 1992; Fewtrell et al., 2003; Link, 2012; Link and Kazakia, 2020).

The theoretical effect of variations in bone size may be explained by using a simple drawing to illustrate the basic physics involved in measurement of BMD with DXA (Binkovitz and Henwood, 2007; Carter et al., 1992; Fewtrell et al., 2003). Fig. 1 shows DXA BMD testing of two cylinders, representing vertebrae of the same height and density but different diameters, scanned as would be in clinical practice; anteroposterior i.e., from front to back. Assuming a homogenous bone cylinder, aBMD is directly proportional to the diameter, whereas vBMD is independent of bone diameter.

1.3. Studies of effects of bone size differences

Studies of healthy adult volunteers have demonstrated the practical effect of bone size on aBMD results (Carter et al., 1992; Chumlea et al., 2002; Colt et al., 2017; Cvijetić and Korsić, 2004; Faulkner et al., 1995; Liao et al., 2004; Srinivasan et al., 2012; Valero et al., 2021). Similarly confounded aBMD results have been reported for adults with Laron Syndrome or Downe Syndrome, where the patients have smaller bones than normal (Benbassat et al., 2003; García-Hoyos et al., 2017).

In children, the effect of variations in bone size between individuals is further complicated by the normal bone growth with increasing age. The effect of anthropometric variables on aBMD results has been studied in children (Baroncelli et al., 1998; Binkovitz and Henwood, 2007; Crabtree et al., 2013; Fewtrell et al., 2003; Gafni and Baron, 2004; Lu et al., 1996; Wren et al., 2005).

In their study of vertebrae from corpses of adult humans, Antonacci et al. (1996) found that variations in bone size significantly affected aBMD results. Ott et al. (1997) studied the bones from young monkeys, finding that aBMD strongly correlated with age as bones changed in size

whereas vBMD did not.

1.4. Mathematical models to correct BMD

Several mathematical models have been proposed to correct for the effect of bone size on aBMD. Carter et al. (1992) developed a general model to use BMAD (Bone Mineral Apparent Density). BMAD was defined as BMC (Bone Mineral Content) / V (bone volume). The BMC was measured as usual, using DXA, and the value of V was calculated from the projected area by assuming the bone to be a specified geometrical shape e.g., a cube. Kröger et al. (1995) compared models for correcting aBMD, using MRI-derived vertebrae dimensions; assuming vertebrae to be cylinders, BMAD was not related to body size. Lu et al. (1996) modelled the central section of the femur as a cylinder, validating the results with measurements on animal femurs.

New models, not relying on representations of bones as a simple geometric shape, continue to be developed. Tatoń et al. (2013) proposed a model that used the ratio of measured vertebral width to depth, to correct for bone size. Luo (2019) used measurements of actual femur bone shape to produce experimental statistical data for corrections to aBMD results. In 2021, Valero et al. used 3-D modelling of bone shape to correct for bone size.

1.5. Confounding effect of soft tissue variations

Although the models have provided corrections to aBMD, to adjust for bone size, they have not taken into account the effect of variations in soft tissues such as fat. Lochmüller et al. (2000) concluded that, because of errors caused by variations in soft tissue surrounding bone, differences in body height and weight and bone size cannot be corrected.

Bolotin (2007) provided an in-depth explanation, of the effect of variations in soft tissue surrounding bone, to support his assertion: *"DXA in vivo BMD: a contaminated and false measure of bone mineral areal density"*. van Rijn and Van Kuijk (2009), cited Bolotin in their discussion on the effect, of change in the amount of fat in growing children, on aBMD results. Colt et al. (2017), also citing Bolotin, concluded that variations
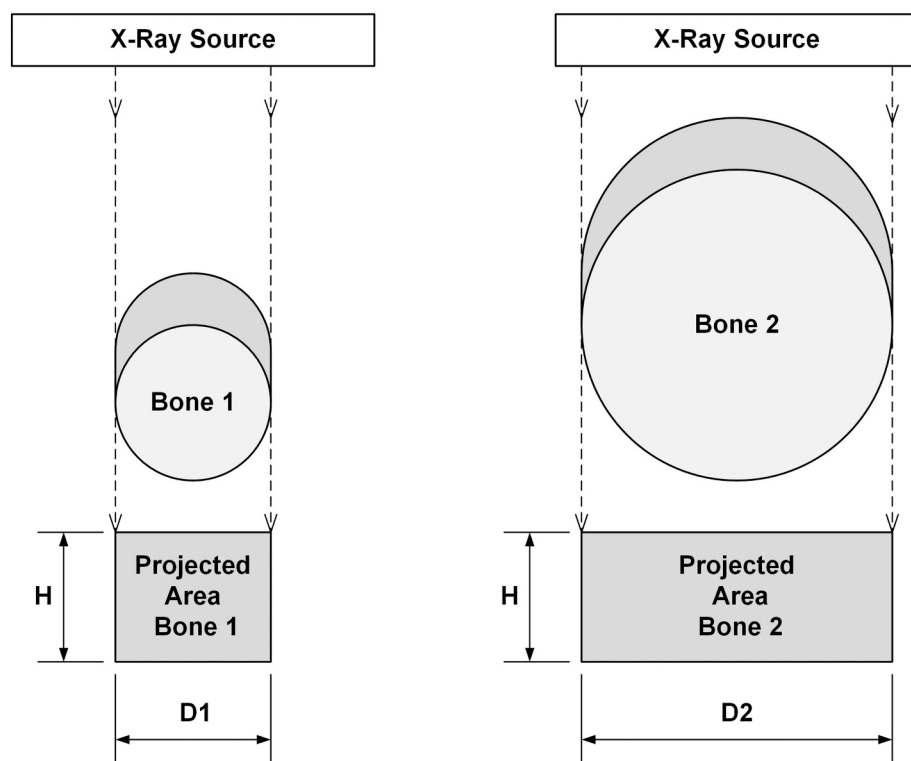

Fig. 1. Effect of bone size on areal density. DXA BMD testing of two cylinders, representing vertebrae of the same height and density but different diameters, scanned as would be in clinical practice; anteroposterior i.e., from front to back.

Assuming a homogenous bone cylinder, DXA aBMD is theoretically directly proportional to the diameter. The linear relationship between aBMD and diameter of two solid cylinders of the same vBMD is derived from first principles in Supplementary Material File SM1.

in fat surrounding bone confounds the results.

1.6. Need for precise, repeatable, quantitative data

Although the dependence of aBMD on bone size is well understood from basic physics theory, and the effect has been repeatedly observed in studies of humans, confirmation of the actual quantitative effect on clinical results for patients requires precise changes in bone size. Studies of humans and animals are limited by the inability to precisely control the size and shape of natural bones.

The objectives of this experiment were to obtain precise, repeatable, quantitative data from sets of artificial vertebrae to confirm the dependence of aBMD on bone size in clinical practice, and to test the effect of applying corrections based on assumptions that the vertebrae were simple geometric shapes.

2. Material and methods

2.1. Experiment design

Four sets of artificial bones, each set containing four cylinders of different diameters, were constructed; all cylinders in all four sets were of identical height (Fig. 2). For convenience of DXA BMD testing, the cylinders are treated as artificial vertebrae L1 to L4 so that all four in a set may be tested in a single scan as would be done for a patient. The X-Ray attenuation of the material used was varied between the sets, to represent differences in BMD. All vertebrae in any one set were made from a single batch of material to ensure that there was no difference in actual BMD.

Each set of vertebrae was tested by placing them in artificial soft tissue, and professionally DXA scanned as would be done in clinical practice; in the anteroposterior position. Because the GE Lunar Prodigy and the Hologic Discovery are the most commonly used DXA scanners used in Australia, the final versions of vertebrae were tested using both instruments.

2.2. Selection of materials for artificial vertebrae

The materials used for the artificial vertebrae were selected to provide a wide range of X-Ray attenuation, to represent a normal range of BMD. The material also needed to be suitable for casting in a mould, and be sufficiently robust to withstand handling during the experiment. It was also essential that the material have very low shrinkage during curing, and able to be precisely ground to size by hand. After trial and error with several materials, a low-viscosity epoxy resin was chosen to provide the structural mass; Aldax Cast Epoxy Casting Resin (Aldax

Enterprises, 2022a and 2022b). The bone mineral analogue was provided by adding finely-ground food-grade calcium carbonate powder (Enfield Produce, 2022) to the epoxy resin.

2.3. Design of artificial vertebrae

The sizes of the vertebrae were chosen to cover the range normally found in humans, based on published data (Zhou et al., 2000). Each set therefore comprises cylinders of diameters 30, 40, 50 and 60 mm, with all having a height of 30 mm.

Details of the calculations for the design of the artificial vertebrae are contained in sheet T1 of Microsoft Excel spreadsheet Supplementary Material file SM2.

The ratio of volume of calcium carbonate to the total (epoxy resin + calcium carbonate) was chosen for each set to provide an R10 Renard Series (Milton, 1978) of mineral concentrations. Commencing at 32 ml calcium carbonate, in each 240 ml batch of material, the amount increased by approximately 25 % for each step to provide the remaining three concentrations of 40, 50 and 63 ml per batch. The total volume of material required was the same for all batches, and was calculated from the sum of volumes of the cylinders plus an allowance for loss in handling.

The materials were to be measured by mass, rather than by volume because it is not possible to accurately measure the volume of calcium carbonate powder, and measuring volumes of epoxy resin would result in errors caused by loss of material; the required amount of each material was therefore converted to mass.

2.4. Construction of artificial vertebrae

A mould was constructed by screwing four models to the base of a two-litre plastic food container, and filling it with Flexicast 65 polyurethane (Barnes, 2022). The four models, identical in size to the designed vertebrae, were professionally precision machined from solid PTFE. To prevent the base of the container from distorting, an acrylic panel was inserted between the underside of the container and the heads of the screws holding the models in place. The entire 2 kg of polyurethane was thoroughly mixed, and poured into the plastic container, and allowed to completely cure before it was removed.

Each set of vertebrae was then constructed by filling each cylindrical hole in the mould with the mixture of epoxy resin and calcium carbonate powder. The masses of each part of the epoxy resin, and the calcium carbonate powder, were measured within 0.1 g using an Ohaus CX1201 digital scale. The calcium carbonate powder was first added to Part A, the least viscous part of the epoxy resin which was also twice the volume of Part B, and mixed thoroughly by hand; Part B was then added and
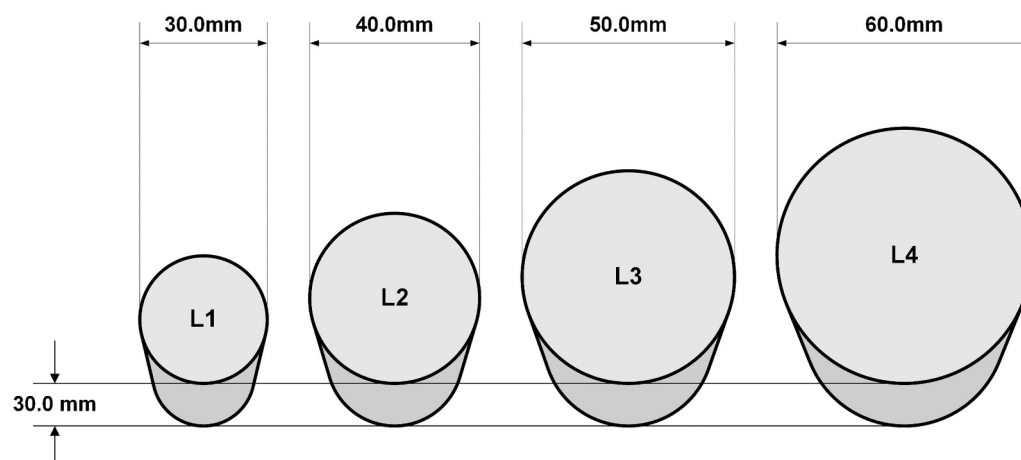

Fig. 2. Vertebrae dimensions.

mixed thoroughly. The first stage of mixing was therefore performed before curing commenced, allowing more time to ensure a homogenous mix of materials.

It was observed that the cast vertebrae initially shrank slightly in height, but not in diameter, soon after casting. To compensate for this, the mould was slightly over-filled. Each cured vertebra was then carefully ground by hand to ensure that all cylinders were of the same finished height.

The models and completed mould and are shown in Fig. 2 of Supplementary Material file SM3.

2.5. Verification testing of artificial vertebrae

To verify that every vertebra in any one set was actually identical in vBMD, their dimensions and mass were precisely measured; dimensions within 0.1 mm using a Mitutoyo Digimatic Caliper; mass within 0.1 g using the Ohaus CX1201 scale. The actual density of each vertebra was calculated from the measured dimensions and mass, and compared to the designed vBMD to verify a linear correlation (Fig. 3). The R^2 was >0.99, so the correlation between measured total density and designed vBMD was very high; this provides a high level of confidence in the quality of the artificial vertebrae.

Details of the calculations for the verification of the artificial vertebrae are contained in sheet T2 of Microsoft Excel spreadsheet Supplementary Material file SM2.

In addition to the quantitative verification, all of the vertebrae were placed in a positioning guide and professionally X-Rayed. The X-Ray image shows the same X-Ray attenuation within each set, and increasing attenuation with increasing calcium carbonate concentration between sets, providing qualitative verification of the quality of the vertebrae.

The four sets of artificial vertebrae in the positioning guide, and the X-Ray image, are shown in Figs. 3 and 4 of Supplementary Material file SM3.

2.6. Design of soft-tissue analogue

The soft tissue was represented by a moulded block of polyurethane in a plastic food container, with a separate top layer of dry rice to cover the vertebrae. The Flexicast 65 (Barnes, 2022) was chosen because it was sufficiently flexible to allow sets of vertebrae to be inserted and removed without damage, and sufficiently rigid to ensure that the vertebrae remained precisely positioned. It was also convenient that this product

was the same as that used to cast the vertebrae.

Testing during development of the artificial vertebrae demonstrated the confounding effect of aBMD sensitivity to variations in soft tissue surrounding bone (refer to 1.5 above). When using a soft-tissue analogue with insufficient X-Ray attenuation, closed-cell polystyrene foam, the DXA scanner was unable to identify the artificial vertebrae.

Rice was chosen on the advice of the staff at the clinic; they used sealed bags of it for patients who had insufficient soft tissue to allow the DXA scanner to correctly identify bones.

2.7. Construction of soft-tissue analogue

The soft-tissue analogue, also used to hold the artificial vertebrae vertically in position, was made by casting the block of polyurethane into a 2-l plastic food container. To produce the half-diameter holes for the cylinders, in the polyurethane block, a spare set of vertebrae was suspended in the container before casting. A hole was drilled through the centre of each spare vertebra and they were spaced along a threaded steel rod that was suspended from holes in the ends of the container. The entire 2 kg of polyurethane was used to cast the soft-tissue analogue. To ensure that all four vertebrae would be adequately covered by dry rice, the fully cured soft-tissue analogue was removed from the 2-l container and placed into a 3-l container having an identical base size but a 50 % greater height.

The construction of the soft-tissue analogue is shown in Figs. 5 to 7 of Supplementary Material file SM3.

The completed soft-tissue analogue, and one set of artificial vertebrae are shown in Fig. 4.

2.8. DXA BMD testing

Each set of vertebrae was scanned, in the anteroposterior position as would be done for a patient, by a radiographer in a clinic. During development of the prototype vertebrae, and for the final versions, the DXA BMD scans were performed using a GE Lunar Prodigy. The scans on the final versions were later also performed on the Hologic Discovery in a different clinic.

Before performing each DXA BMD scan on a set, each vertebra was pressed by hand into the matching half-cylinder hole in the top of the polyurethane block (Fig. 4). One kg of dry rice was then added to the container to complete the soft-tissue analogue. After scanning was completed for each set of vertebrae, all of the rice was poured out of the
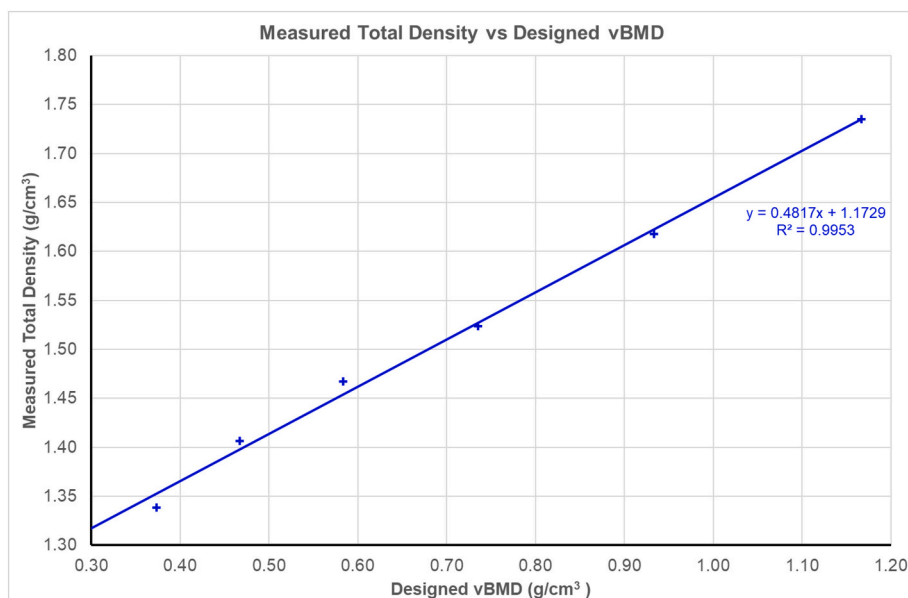

Measured Total Density vs Designed vBMD

$y = 0.4817x + 1.1729$
$R^2 = 0.9953$

Fig. 3. Measured vertebrae total density vs designed vBMD. Vertebrae sets CC80 and CC100 were not included for DXA BMD measurements, in testing of final version of vertebrae because, during preliminary testing, their aBMD was higher than the range of interest and non-linear with the designed vBMD.

The measured total density for each set of vertebrae is plotted against the designed vBMD for that set. With an r^2 of 0.9953, measured vertebrae total density and designed total density are very highly correlated. This verifies that the actual ratio of materials for each set is consistent with the designed linear increase in actual BMD (Renard R10 series) from lowest to highest concentration.

Fig. 4. One set of vertebrae installed in soft-tissue analogue. The lid is attached after the dry rice is poured into the container; the dashed lines on the lid label form a target for precise alignment of the vertebrae with the cross-hairs of the DXA scanner.

container and the vertebrae were pulled out of the polyurethane block by hand.

Because the scans were completed more quickly than expected, on the Hologic Discovery, the remaining scanner time allocated was used to perform two repeat scans on all four sets of vertebrae.

3. Results

3.1. Result reports - GE lunar prodigy

The aBMD results reports for the artificial vertebrae, from the GE Lunar Prodigy, are contained in PDF Supplementary Material file SM4.

There is a single results page for each of the four sets of artificial vertebrae. The calcium carbonate concentration of the set may be identified from the Patient ID e.g., CC32 contains 32 ml bone mineral analogue per 240 ml. Each page contains an X-Ray image of the four vertebrae, L1 to L4, and a table of results with aBMD and the T and Z scores; projected area and BMC were not included. The only results data extracted for this scanner was the value of aBMD for each vertebra.

3.2. Result reports - hologic discovery

The DXA BMD results reports for the artificial vertebrae, from the Hologic Discovery, are contained in PDF Supplementary Material file SM5.

Because the scans were repeated twice for this scanner, there are three pages of results for each set of vertebrae. In addition to the same data provided by the GE Lunar Prodigy, aBMD and the T and Z scores, the results table included projected area and BMC. The results data extracted for this scanner were the value of aBMD, projected area and BMC for each vertebra.

3.3. Analysis of BMD results

The aBMD results from the GE Lunar Prodigy and the Hologic Discovery were analysed using Microsoft Excel; the spreadsheet file is Supplementary Material SM6.

The designed, measured and calculated physical properties were copied from Table 2 of SM2 to Table 1 of SM6. The aBMD result for each vertebra was transcribed, from the DXA BMD reports (SM4 and SM5), into Table 1 of SM6. For the Hologic Discovery, the projected area and BMC for each vertebra were also included.

The three aBMD results for each vertebra, from the Hologic Discovery, were averaged to reduce the effect of random errors. There was no

formal quantitative analysis of the spread of the three sets of aBMD results because it was outside the scope of the experiment; producing meaningful statistical data would have required significantly more repeated tests.

A graphical analysis, of the spread of results has been provided in chart C10 of SM6. This chart shows each of the three individual aBMD measurements, for each vertebra in each set, plotted as a short horizontal black bar onto the graph of Reported aBMD vs Measured Diameter. The vertical spread of the black bars, around the regression line for each set of vertebrae, is a measure of the repeatability of the aBMD results. The spread of results for the CC50 5.0 cm and CC50 6.0 cm vertebrae, and the CC63 6.0 cm vertebra are greater than the others, but there is insufficient data to conclude that there is any statistically significant increase in the spread with either the mineral density or diameter. It is possible that the observed spread of results is indicative of the limitations of the edge detection precision of the Hologic Discovery.

The effect of change in bone diameter on aBMD and BMAD, is shown in the charts contained in Figs. 5 to 8. The significance of the effect of applying the BMAD corrections for cube and cylinder is shown in Fig. 9.

The four graphed series on each chart in Figs. 5 to 8 (CC32, CC40, CC50 and CC63) are for each of the sets of vertebrae in the Renard R10 series of increasing calcium carbonate concentration. The regression line has been plotted, and the linear equation is given on the charts in the form: $y = mx + b$, where y is the BMD for each diameter x, m is the slope and b is the offset. The square of the regression coefficient, for each set of vertebrae, is also given on each chart.

To compare the effect of bone diameter on aBMD, to the effect on BMAD for a cube or a cylinder, it was necessary to perform additional analyses. If the variables aBMD and BMAD were in the same units, the effect of bone diameter on BMD could have been directly expressed as the slope of the graph of BMD vs diameter. Because aBMD is in units of g/cm^2, and BMAD is in units of g/cm^3, the slopes of the graphs cannot be validly directly compared; another step is required.

By calculating the ratio of the slope and the offset of the graph for each set of vertebrae, it is possible to eliminate the units and obtain a proportional change. It is thereby valid to compare the change in BMD with change in bone diameter, for aBMD and BMAD for cube or cylinder. The calculations for these analyses are contained in Table 2 of SM6.

3.4. Effect of change in bone diameter on DXA BMD (aBMD)

The effect of change in bone diameter on aBMD was analysed by plotting reported aBMD against measured diameter, for each vertebra for each set of vertebrae, for each scanner (Fig. 5). For both DXA scanners, for all four sets of vertebrae, the reported increase in aBMD is directly proportional to the increase in bone diameter. The R^2 was >0.99, for each set of vertebrae for both scanners, so the correlation between aBMD and diameter was very high; this provides a high level of confidence in the results.

3.5. Quantitative relationship between DXA BMD (aBMD) and vertebrae diameter

The analysis of correlation between aBMD and bone diameter, in 3.4 above, is not sufficient to verify the theoretical direct proportionality between them (as derived from first principles in Fig. 1). This is because correlation is not a measure of the significance of a change in a dependent variable compared to an initial value of that variable.

What is required is a measure of the significance of a change in aBMD, for each change in diameter, compared to any offset in the value of aBMD for the initial diameter. To quantify the relationship for each diameter, for each set of vertebrae, it is necessary to compare two ratios for each vertebra: the ratio of aBMD to that of the aBMD for the vertebra with the initial (smallest) diameter; the ratio of vertebra diameter to that of the initial diameter. The ratios of aBMD vs ratios of diameters, for each set of vertebrae, are plotted in Fig. 6.
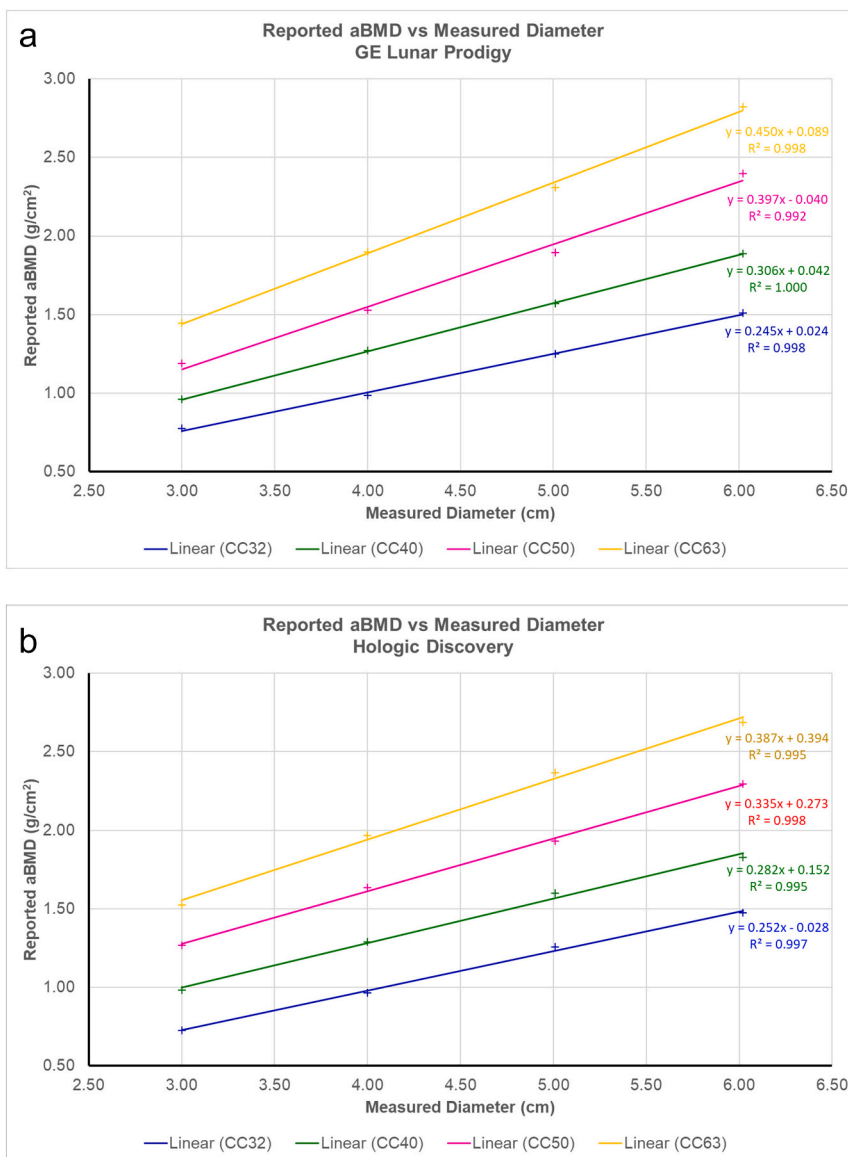
Fig. 5. aBMD vs measured diameter. a: GE Lunar Prodigy. b: Hologic Discovery.

For the GE Lunar Prodigy, for each set of vertebrae, the ratio of increase in aBMD to offset is very highly correlated with the ratio of increase in diameter; the R^2 was >0.99. From the linear equations in Fig. 6a, for each set of vertebrae, the rate of change of aBMD with diameter (m in the linear equation y = mx + b) is more than an order of magnitude greater than the offset (b in the equation). Also, from the graph and linear equation for each set of vertebrae, the aBMD of the 6.0 cm diameter vertebrae were within a range of 1.950 to 2.020 times the aBMD of the 3.0 cm vertebrae. This is consistent with the theoretical increase of 2.0 times for direct proportionality between aBMD and diameter.

For the Hologic Discovery, the ratio of increase in aBMD to offset is also very highly correlated with the ratio of increase in diameter; the R^2 was >0.99. From the linear equations in Fig. 6b, for the two sets of vertebrae with the lower calcium carbonate concentrations (sets CC32 and CC40), the rate of change of aBMD with diameter is more than an order of magnitude greater than the offset. For the two sets of vertebrae with the higher calcium carbonate concentrations (sets CC50 and CC63), the rate of change of aBMD with diameter is far less than an order of magnitude greater than the offset. This anomaly, between the sets of vertebrae, is also visually apparent from the significant variations, in the

slopes of the regression lines. From the graph, the ratio of aBMD of the 6.0 cm diameter vertebrae, to the 3.0 cm vertebrae, falls from 2.028 to 1.765 with increasing calcium carbonate concentrations.

3.6. Effect of bone diameter on BMAD for a cube

The effect of bone diameter on BMAD for a cube was analysed by plotting the calculated BMAD against measured diameter, for each vertebra for each set of vertebrae, for each scanner (Fig. 7). The BMAD for a cubic AP projection (vcBMD) was calculated from the BMC and volume of the cubic anteposterior projection. For the Hologic Discovery, the reported BMC was used. Because BMC was not reported for the GE Lunar Prodigy, the BMC was calculated from the reported aBMD and calculated AP area.

For BMAD for a cube, the significance of an effect of change of bone diameter may be seen from the ratio of the slope to offset of the regression line for each set of vertebrae (second set of columns in Fig. 9). By comparing these ratios to those for aBMAD (first set of columns in Fig. 9) it may be seen that the change, from aBMD to BMAD for a cube, has reduced the effect of change in bone diameter by approximately one order of magnitude for both scanners.
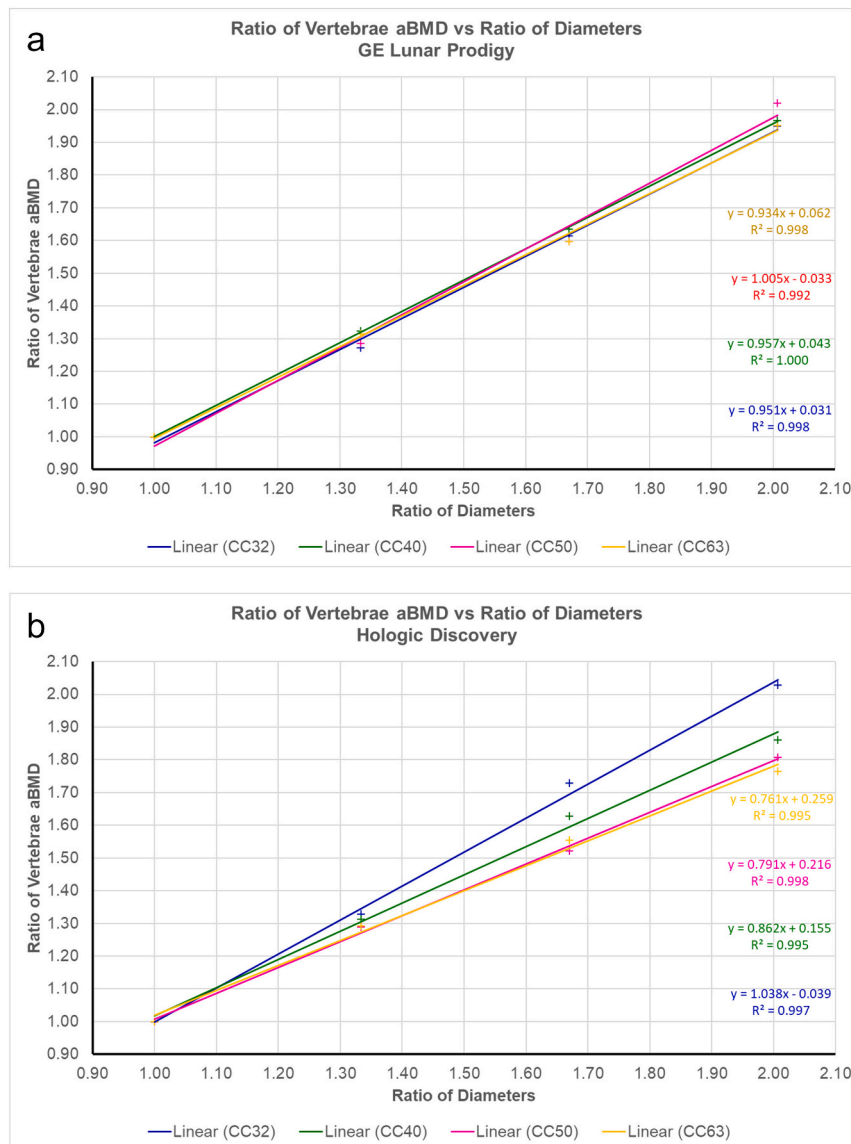
Fig. 6. Ratio of Vertebrae aBMD vs Ratio of Diameters a: GE Lunar Prodigy. b: Hologic Discovery.

For all four sets of vertebrae, the reported cubic BMAD is still directly proportional to bone diameter, for both scanners. For the GE Lunar Prodigy, the R^2 was >0.98, for each set of vertebrae, so the correlation between cubic BMAD and diameter was not significantly less than for the aBMD results. For the Hologic Discovery, the R^2 ranged from 0.84 to 0.99 between sets of vertebrae, so the correlation between cubic BMAD and diameter was slightly less than for the aBMD results.

The BMAD correction for a cube does not eliminate the change of aBMD with diameter because the Carter model (Carter et al., 1992) assumes that the vertebra height increases with width. The volume of the cubic projection is calculated by cubing the square root of the area i.e., it is assumed that the length of the sides of the cube are changing as the height of the vertebra changes. In the case of the cylindrical vertebrae used in this experiment, the height is constant for all vertebra regardless of the diameter.

3.7. Effect of bone diameter on BMAD for a cylinder

The effect of bone diameter on BMAD for a cylinder was analysed by plotting the calculated BMAD against measured diameter, for each vertebra for each set of vertebrae, for each scanner (Fig. 8). The BMAD

for a cylindrical AP projection (vrBMD) was calculated similarly to the BMAD for a cube, as above.

For BMAD for a cylinder, the significance of an effect of change of bone diameter may be seen from the ratio of the slope to offset of the regression line for each set of vertebrae (Third set of columns in Fig. 9). By comparing these ratios to those in the first set of columns, it may be seen that the change, from aBMD to BMAD for a cylinder, has reduced the effect of change in bone diameter by approximately two orders of magnitude for both scanners.

For both DXA scanners, for all four sets of vertebrae, the BMAD for a cylinder is not significantly affected by bone diameter.

3.8. BMD vs designed vBMD

In addition to the initial verification testing of the artificial vertebrae (refer to 2.5 above), further quality control checks were made after performing the DXA BMD tests. The reported aBMD, and the derived BMAD for cube and cylinder, were plotted against the designed vBMD for each set of artificial vertebrae, for the GE Lunar Prodigy and the Hologic Discovery.

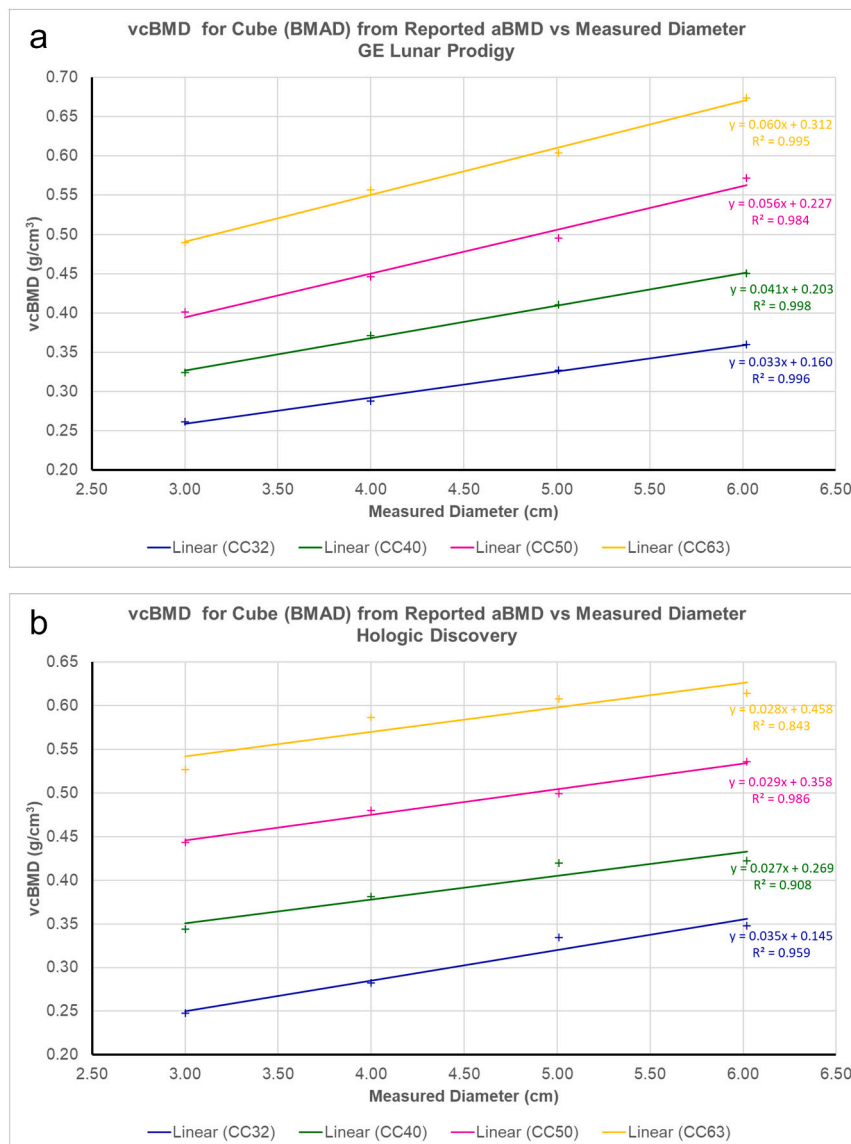For both DXA scanners, the R^2 was >0.98, for each set of vertebrae,

Fig. 7. vcBMD for cube (BMAD) from reported aBMD vs measured diameter. a: GE Lunar Prodigy. b: Hologic Discovery.

so the correlation between the reported aBMD and designed vBMD was very high; this verifies the quality of the artificial vertebrae and the validity of the method. The data tables and charts are contained in Tables 1 and 3, and Charts 5 to 7, of SM6.

4. Discussion and conclusion

4.1. Validity of using artificial bones

By precisely controlling each stage of the construction, and by quantitatively verifying their quality, it has been possible to produce artificial vertebrae covering the complete range of sizes and mineral densities found in human bones. Results obtained from these artificial bones are repeatable, and more complex shapes could be produced by advanced techniques such as 3-D printing to test newer mathematical models.

4.2. Verification of theoretical direct proportionality between aBMD and diameter

The aBMD results from the GE Lunar Prodigy, for all four sets of

vertebrae, verify the theoretical direct proportionality between aBMD and diameter. For the two sets of vertebrae with the lower concentrations of calcium carbonate, the results from the Hologic Discovery are similarly consistent with the theory.

Although the change in aBMD reported by the Hologic Discovery is highly correlated with change in diameter, for all sets of vertebrae, the value of aBMD is not directly proportional to diameter for the two sets with higher concentrations of calcium carbonate; there is a significant offset of the aBMD compared to the rate of change. This anomaly might be caused by differences in the scanning technique used by the instruments; the GE Lunar Prodigy uses a narrow-angle fan beam, whereas the Hologic Discovery uses a wide-angle fan beam.

4.3. Dependence of DXA BMD on bone size in clinical practice

By obtaining precise, repeatable, quantitative data from sets of artificial vertebrae, this experiment has confirmed that aBMD results are affected by bone size in clinical practice. The aBMD results from the GE Lunar Prodigy and the Hologic Discovery are not in any way corrected for differences in bone size. This is likely to be a significant factor contributing to false positives (overdiagnosis) for patients with small
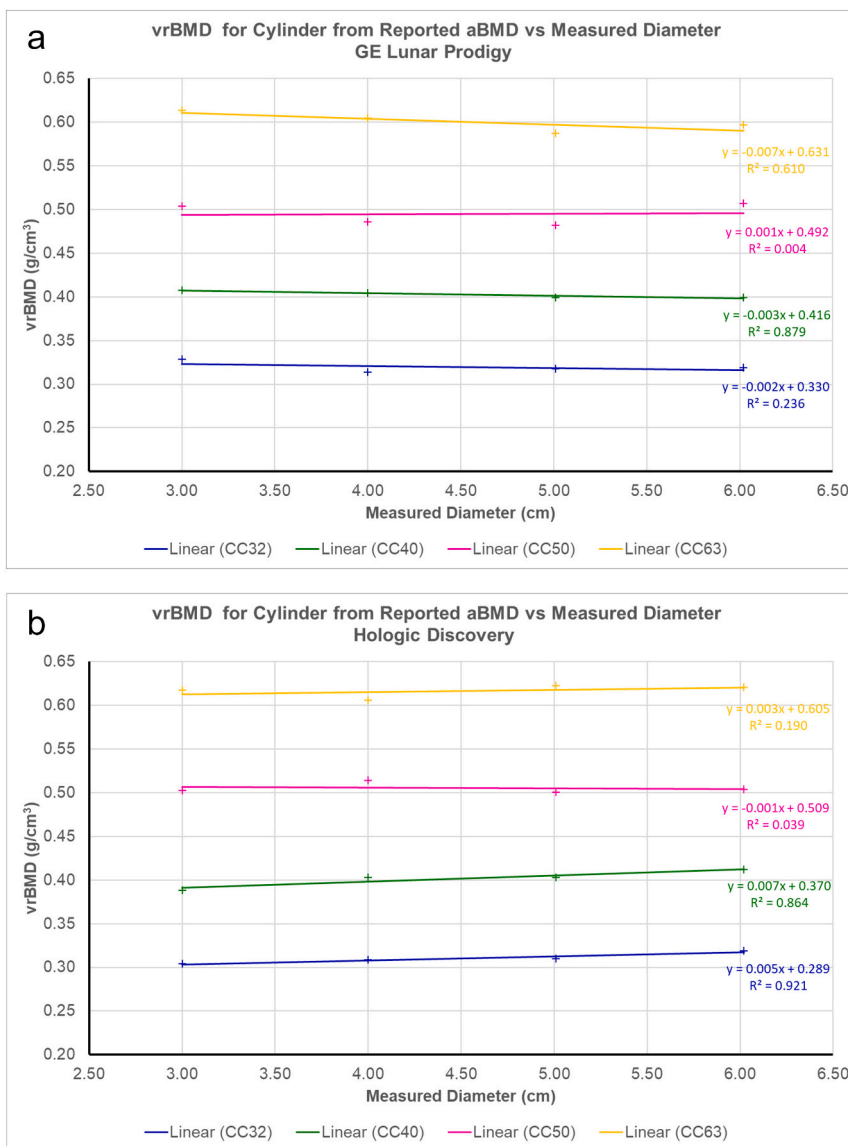
Fig. 8. vrBMD for cylinder (BMAD) from reported aBMD vs measured diameter. a: GE Lunar Prodigy. b: Hologic Discovery.

bones, and false negatives (underdiagnosis) for patients with large bones.

4.4. Effectiveness of mathematical BMAD models to correct reported BMD

By comparing the ratio of slope to offset of the regression lines for BMD vs diameter, for uncorrected aBMD to BMAD for cube and BMAD for cylinder, this experiment has confirmed the validity of applying these corrections to simple solid geometrical shapes. The elimination of any significant effect of change in bone size, when aBMD was corrected for a cylinder, was consistent with the theoretical outcome.

4.5. Limitations of the experiment

There are limitations to the ability of these artificial cylinders to represent natural bones: they are solid and homogenous, whereas natural bones are neither solid nor homogenous; they are simple geometrical shapes, whereas natural bones are complex shapes; they are embedded in a homogenous soft-tissue analogue, whereas soft tissue surrounding natural bones can be highly variable.

4.6. Conclusion

This experiment has confirmed that BMD measured using DXA, accepted in clinical practice as the *"gold standard"* means of diagnosing osteoporosis, could lead to misdiagnosis because it is significantly affected by differences in bone size.

Supplementary data to this article can be found online at https://doi.org/10.1016/j.bonr.2022.101607.

CRediT authorship contribution statement

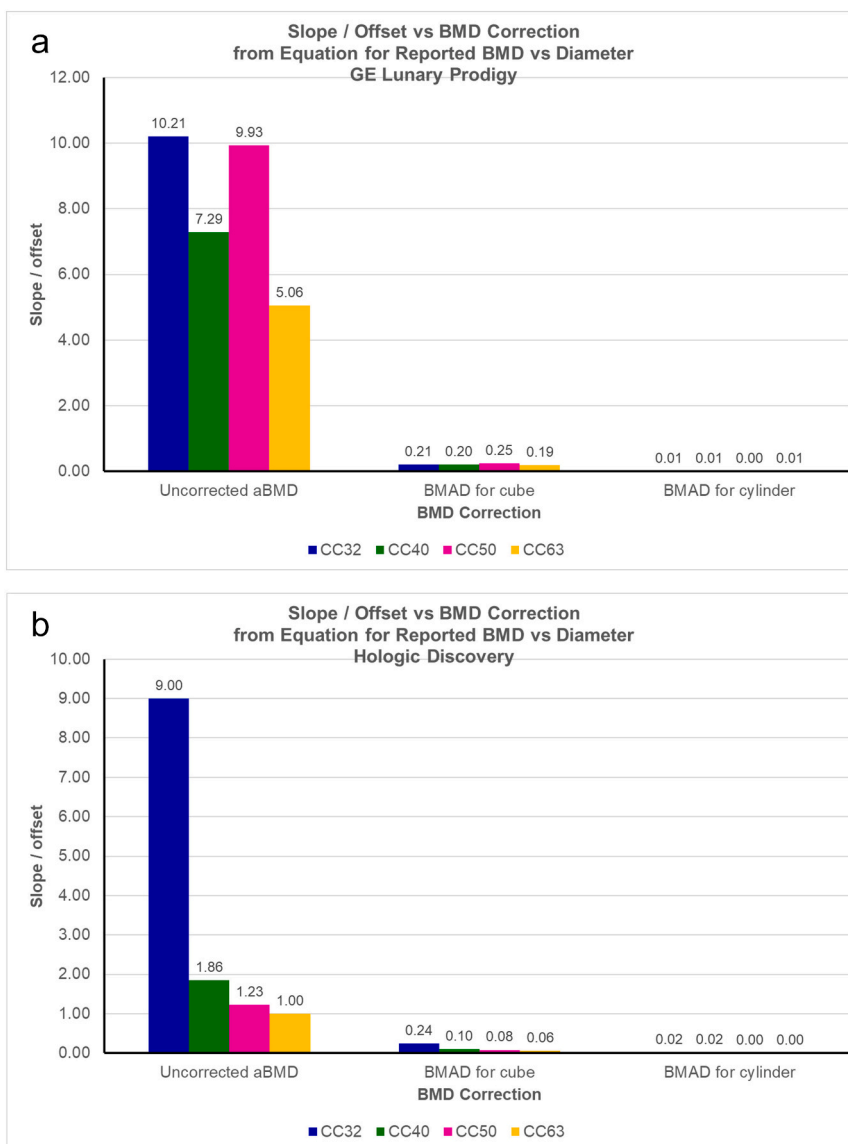The sole author was responsible for all aspects of the experiment and the manuscript.

Fig. 9. Slope/Offset vs BMD correction from equation for reported BMD vs diameter a: GE Lunar Prodigy. b: Hologic Discovery.

References

Aldax Enterprises, 2022. Aldax Cast Epoxy Casting Resin Part A Material Safety Data Sheet. http://www.aldax.com.au/msds_tds/msds/Aldax%20Crystal%20Cast%20Epoxy%20Casting%20Resin%20Part%20A.pdf (accessed 28 March 2022).

Aldax Enterprises, 2022. Aldax Cast Epoxy Casting Resin Part B Material Safety Data Sheet. http://www.aldax.com.au/msds_tds/msds/Aldax%20Crystal%20Cast%20Epoxy%20Casting%20Resin%20Part%20B.pdf (accessed 28 March 2022).

Antonacci, M.D., Hanson, D.S., Heggeness, M.H., 1996. Pitfalls in the measurement of bone mineral density by dual energy x-ray absorptiometry. Spine 21 (1), 87–91. https://doi.org/10.1097/00007632-199601010-00020.

Barnes, 2022. Flexicast 65 technical data sheet. https://www.barnes.com.au/wp-content/uploads/myintegrator/documents/FLEXICAST%2065.pdf accessed 28 March 2022.

Baroncelli, G.I., Bertelloni, S., Ceccarelli, C., Saggese, G., 1998. Measurement of volumetric bone mineral density accurately determines degree of lumbar undermineralization in children with growth hormone deficiency. J. Clin. Endocrinol. Metab. 83 (9), 3150–3154. https://doi.org/10.1210/jcem.83.9.5072.

Benbassat, C.A., Eshed, V., Kamjin, M., Laron, Z., 2003. Are adult patients with laron syndrome osteopenic? A comparison between dual-energy X-ray absorptiometry and volumetric bone densities. J. Clin. Endocrinol. Metab. 88 (10), 4586–4589. https://doi.org/10.1210/jc.2003-030623.

Binkovitz, L.A., Henwood, M.J., 2007. Pediatric DXA: technique and interpretation. Pediatr. Radiol. 37 (1), 21–31. https://doi.org/10.1007/s00247-006-0153-y.

Bolotin, H.H., 2007. DXA in vivo BMD methodology: an erroneous and misleading research and clinical gauge of bone mineral status, bone fragility, and bone remodelling. Bone 41 (1), 138–154. https://doi.org/10.1016/j.bone.2007.02.022.

Carter, D.R., Bouxsein, M.L., Marcus, R., 1992. New approaches for interpreting projected bone densitometry data. J. Bone Miner. Res. Off. J. Am. Soc. Bone Miner. Res. 7 (2), 137–145. https://doi.org/10.1002/jbmr.5650070204.

Chumlea, W.C., Wisemandle, W., Guo, S.S., Siervogel, R.M., 2002. Relations between frame size and body composition and bone mineral status. Am. J. Clin. Nutr. 75 (6), 1012–1016. https://doi.org/10.1093/ajcn/75.6.1012.

Colt, E., Akram, M., Pi Sunyer, F., 2017. Comparison of high-resolution peripheral quantitative computerized tomography with dual-energy X-ray absorptiometry for measuring bone mineral density. Eur. J. Clin. Nutr. 71, 778–781. https://doi.org/10.1038/ejcn.2016.178.

Crabtree, N.J., Högler, W., Cooper, M.S., Shaw, N.J., 2013. Diagnostic evaluation of bone densitometric size adjustment techniques in children with and without low trauma fractures. Osteoporos. Int. 24 (7), 2015–2024. https://doi.org/10.1007/s00198-012-2263-8.

Cvijetić, S., Korsić, M., 2004. Apparent bone mineral density estimated from DXA in healthy men and women. Osteoporos. Int. 15 (4), 295–300. https://doi.org/10.1007/s00198-003-1525-x.

Enfield Produce, 2022. Specification Calcium Carbonate FCC/JECFA. https://www.petandgarden.com.au/index.php?controller=attachment&id_attachment=78 (accessed 28 March 2022).

Faulkner, R.A., McCulloch, R.G., Fyke, S.L., De Coteau, W.E., McKay, H.A., Bailey, D.A., Houston, C.S., Wilkinson, A.A., 1995. Comparison of areal and estimated volumetric bone mineral density values between older men and women. Osteoporos. Int. 5 (4), 271–275. https://doi.org/10.1007/BF01774017.

Fewtrell, M.S., British Paediatric &amp, Adolescent Bone Group, 2003. Bone densitometry in children assessed by dual x ray absorptiometry: uses and pitfalls. Arch. Dis. Childhood 88 (9), 795–798. https://doi.org/10.1136/adc.88.9.795.

Gafni, R.I., Baron, J., 2004. Overdiagnosis of osteoporosis in children due to misinterpretation of dual-energy x-ray absorptiometry (DEXA). J. Pediatr. 144 (2), 253–257. https://doi.org/10.1016/j.jpeds.2003.08.054.

García-Hoyos, M., García-Unzueta, M.T., de Luis, D., Valero, C., Riancho, J.A., 2017. Diverging results of areal and volumetric bone mineral density in down syndrome. Osteoporos. Int. 28 (3), 965–972. https://doi.org/10.1007/s00198-016-3814-1.

Henry, M.J., Pasco, J.A., Korn, S., Gibson, J.E., Kotowicz, M.A., Nicholson, G.C., 2010. Bone mineral density reference ranges for australian men: Geelong osteoporosis study. Osteoporos. Int. 21 (6), 909–917. https://doi.org/10.1007/s00198-009-1042-7.

Kröger, H., Vainio, P., Nieminen, J., Kotaniemi, A., 1995. Comparison of different models for interpreting bone mineral density measurements using DXA and MRI technology. Bone 17 (2), 157–159. https://doi.org/10.1016/s8756-3282(95)00162-x.

Liao, E.Y., Wu, X.P., Liao, H.J., Zhang, H., Peng, J., 2004. Effects of skeletal size of the lumbar spine on areal bone density, volumetric bone density, and the diagnosis of osteoporosis in postmenopausal women in China. J. Bone Miner. Metab. 22 (3), 270–277. https://doi.org/10.1007/s00774-003-0479-6.

Link, T.M., 2012. Osteoporosis imaging: state of the art and advanced imaging. Radiology 263 (1), 3–17. https://doi.org/10.1148/radiol.2631201201.

Link, T.M., Kazakia, G., 2020. Update on imaging-based measurement of bone mineral density and quality. Curr. Rheumatol. Rep. 22 (5), 13. https://doi.org/10.1007/s11926-020-00892-w.

Lochmüller, E.M., Miller, P., Bürklein, D., Wehr, U., Rambeck, W., Eckstein, F., 2000. In situ femoral dual-energy X-ray absorptiometry related to ash weight, bone size and density, and its relationship with mechanical failure loads of the proximal femur. Osteoporos. Int. 11 (4), 361–367. https://doi.org/10.1007/s001980070126.

Lu, P.W., Cowell, C.T., LLoyd-Jones, S.A., Briody, J.N., Howman-Giles, R., 1996. Volumetric bone mineral density in normal subjects, aged 5-27 years. J. Clin.

Endocrinol. Metab. 81 (4), 1586–1590. https://doi.org/10.1210/jcem.81.4.8636372.

Luo, Y., 2019. Empirical functions for conversion of femur areal and volumetric bone mineral density. J. Med. Biol. Eng. 39, 287–293. https://doi.org/10.1007/s40846-018-0394-x.

Milton, H., 1978. The selection of preferred metric values for design and construction. In: National Bureau of Standards, US Department of Commerce, pp. 29–31 (accessed 20 April 2022). https://www.govinfo.gov/content/pkg/GOVPUB-C13-f5fea679df4c3a1c2e3e1dd63488707c/pdf/GOVPUB-C13-f5fea679df4c3a1c2e3e1dd63488707c.pdf.

Ott, S.M., O'Hanlan, M., Lipkin, E.W., Newell-Morris, L., 1997. Evaluation of vertebral volumetric vs. Areal bone mineral density during growth. Bone 20 (6), 553–556. https://doi.org/10.1016/s8756-3282(97)00057-4.

Srinivasan, B., Kopperdahl, D.L., Amin, S., Atkinson, E.J., Camp, J., Robb, R.A., Riggs, B.L., Orwoll, E.S., Melton 3rd, L.J., Keaveny, T.M., Khosla, S., 2012. Relationship of femoral neck areal bone mineral density to volumetric bone mineral density, bone size, and femoral strength in men and women. Osteoporos. Int. 23 (1), 155–162. https://doi.org/10.1007/s00198-011-1822-8.

Tatoń, G., Rokita, E., Wróbel, A., Korkosz, M., 2013. Combining areal DXA bone mineral density and vertebrae postero-anterior width improves the prediction of vertebral strength. Skelet. Radiol. 42 (12), 1717–1725. https://doi.org/10.1007/s00256-013-1723-3.

Valero, C., Olmos, J.M., Humbert, L., Castillo, J., Hernández, J.L., Martínez, J., Martínez, J.G., 2021. 3D analysis of bone mineral density in a cohort: age- and sex-related differences. Arch. Osteoporos. 16, 80. https://doi.org/10.1007/s11657-021-00921-w.

van Rijn, R.R., Van Kuijk, C., 2009. Of small bones and big mistakes; bone densitometry in children revisited. Eur. J. Radiol. 71 (3), 432–439. https://doi.org/10.1016/j.ejrad.2008.08.017.

WHO Scientific Group, 2007. WHO Technical Report; Assessment of Osteoporosis at the Primary Health Care Level. World health Organization. https://www.sheffield.ac.uk/FRAX/pdfs/WHO_Technical_Report.pdf (accessed 7 April 2022).

WHO Scientific Group, 2003. WHO Technical Report 921; Prevention and management of osteoporosis. World Health Organization. https://apps.who.int/iris/bitstream/handle/10665/42841/WHO_TRS_921.pdf?sequence=1&isAllowed=y (accessed 7 April 2022).

Wren, T.A., Liu, X., Pitukcheewanont, P., Gilsanz, V., 2005. Bone acquisition in healthy children and adolescents: comparisons of dual-energy x-ray absorptiometry and computed tomography measures. J. Clin. Endocrinol. Metab. 90 (4), 1925–1928. https://doi.org/10.1210/jc.2004-1351.

Zhou, S.H., McCarthy, I.D., McGregor, A.H., Coombs, R.R., Hughes, S.P., 2000. Geometrical dimensions of the lower lumbar vertebrae–analysis of data from digitised CT images. Eur. Spine J. 9 (3), 242–248. https://doi.org/10.1007/s005860000140.